JOURNAL OF CATALYSIS 147, 5–14 (1994)

In Situ Diffuse Reflectance FTIR Study of the Selective Catalytic Reduction of NO by NH_3 over Vanadia–Titania Aerogels

H. Schneider,* S. Tschudin,* M. Schneider,* A. Wokaun,† and A. Baiker*,[1]

*Department of Chemical Engineering and Industrial Chemistry, Swiss Federal Institute of Technology, ETH-Zentrum, CH-8092 Zürich, Switzerland; and †Physical Chemistry II, University of Bayreuth, D-95440 Bayreuth, Germany

Received September 10, 1993; revised December 7, 1993

Selective catalytic reduction of NO by NH_3 (SCR) on high surface area (BET > 180 $m^2\ g^{-1}$ vanadia–titania aerogels with 5, 10, and 20 wt% of vanadia, has been investigated by diffuse reflectance FTIR spectroscopy coupled with mass spectrometry under reaction conditions and by temperature-programmed desorption of preadsorbed NH_3 and NO. The SCR activity of these catalysts increases with the vanadia loading. This behaviour is reflected by the temperatures necessary to reach 50% NO conversion under standard conditions, which decreased in the sequence 5% V_2O_5, 545 K; 10% V_2O_5, 470 K; 20% V_2O_5, 440 K. A similarly prepared high surface area (182 $m^2\ g^{-1}$) titania aerogel does not exhibit significant NO conversion in this temperature range. On pure titania aerogel, mainly Lewis-bound ammonia is observed subsequent to NH_3 adsorption at ambient temperature. In contrast, it is shown that Brønsted-bound ammonia, characterized by bands at 1660 and 1414 cm^{-1}, is involved in the SCR reaction. The SCR activities correlate with the fraction of Brønsted-bound ammonia which significantly increases with the vanadia loading of the aerogel samples.

INTRODUCTION

Initiated by its environmental importance, the selective catalytic reduction (SCR) of NO_x by NH_3 has been studied intensively, and various reaction mechanisms have been proposed (1). Based on IR spectroscopy studies Takagi *et al.* (2, 3) proposed a Langmuir–Hinshelwood mechanism involving NO, adsorbed as $NO_2(O_s + NO)$, and NH_3 adsorbed as NH_4^+.

Imomata *et al.* (4) deduced from gas chromatography and IR spectroscopy investigations that NH_4^+ acts as the active ammonia species and reacts with NO from the gas phase according to an Eley–Rideal mechanism. Janssen *et al.* (5) further supported this mechanism by isotopic transient studies with $^{18}O_2$ and $^{15}N_2$, which indicated that ammonia does not react with O_2 or O from any source during the reaction, and that nitrogen and nitrous oxide are produced by a reaction involving all three species: NO, NH_3, and/or O_2. Chen and Yang (6) supported this suggestion using alkali metals to poison Brønsted acid sites, which were suggested to be the active sites for the SCR reaction.

Gasior *et al.* (7) concluded from XPS measurements on single-crystal surfaces of V_2O_5 as well as from IR measurements that the SCR reaction proceeds via participation of ammonia adsorbed on Brønsted acid sites.

Odriozola *et al.* (8) confirmed this suggestion by Auger electron spectroscopy and thermal desorption spectroscopy studies. They showed that NO adsorbs only on titania and on reduced vanadia, but not on oxidized vanadia surfaces. It was also shown that ammonia reduces the vanadium pentoxide, thereby yielding N_2O. Although the authors did not find evidence for the SCR reaction over the titania surface they proposed NO adsorption *on titania* to be an important step in the catalytic action of vanadia/titania.

According to Ramis *et al.* (9), the reaction proceeds via ammonia adsorbed on Lewis sites of the vanadia. This mechanism is in contrast to those described above. Although there are a number of studies dealing with the adsorption of ammonia on vanadia (10–20), there is still an ongoing debate about the active site in the SCR reaction, mainly due to the fact that in most investigations (10–14, 17, 19, 20) the structure of the adsorbed reactants and kinetics could not be followed simultaneously.

In the present work we have used diffuse reflectance FTIR (DRIFT) combined with mass spectrometry to characterize the active surface species involved in the SCR of NO. Vanadia–titania aerogel catalysts with extremely high surface areas were used for obtaining optimal spectral resolution. Dynamic and steady-state measurements under SCR conditions were applied to elucidate the nature of the active sites.

[1] To whom correspondence should be addressed.

0021-9517/94 $6.00

EXPERIMENTAL

Catalysts

Four types of aerogels have been used, pure titania and mixed vanadia–titania containing 5, 10, and 20 wt% of vanadia (nominally V_2O_5). The preparation of the titania gels both for the titania and the binary aerogels basically followed that of aerogel C in (21). In brief, tetrabutoxytitanium(IV) was dissolved in methanol. The subsequent addition of the acid hydrolysant diluted in methanol resulted in a gel. The as-prepared titania gels were aged and thereafter redispersed with an extra amount of methanol. In order to synthesize the vanadia–titania mixed gels various amounts of vanadium(V) tri-*n*-propoxide oxide also diluted in methanol were added under vigorous stirring. After a second ageing step, these solutions were transferred into an autoclave and dried under supercritical conditions in a batch operation at 533 K. Finally, the aerogel materials were ground to a fine powder and calcined in flowing air at 573 K for 5 h. The detailed preparation and structural characterization of the vanadia–titania aerogels will be described elsewhere (22).

Apparatus and Procedures

The temperature-programmed desorption (TPD) studies were carried out using an apparatus (Fig. 1) consisting essentially of a gas dosing system, an FTIR instrument (Perkin–Elmer, model 1710) equipped with a DRIFT cell (environmental chamber, Starna, model HCV-D3), and a mass spectrometer (Balzers QMG 420, 6 × 125-mm system, software Quadstarplus). For the DRIFT studies the aerogel powder containing particles smaller than 50 μm was placed in a glass stewpan with a sintered plate on the bottom such that the gas passed through the catalyst powder. The temperature of the catalyst bed was measured with a Cr/CrNi thermocouple, and controlled to an accuracy of ±3 K. As in the DRIFT cell the thermocouple is located in the heated steel stand; the temperature of the

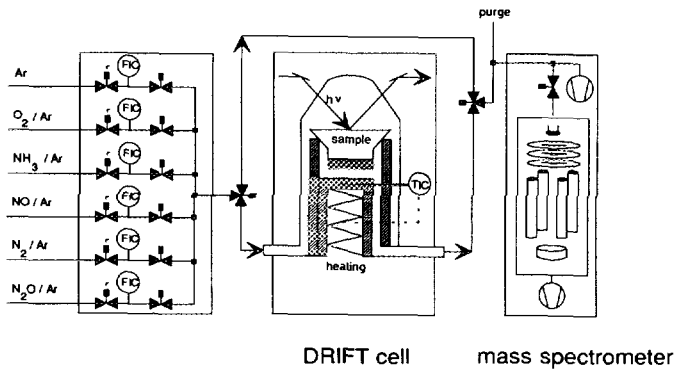

FIG. 1. Flow scheme of the apparatus consisting of the gas dosing system (FIC, mass flow controllers), the *in situ* diffuse reflectance cell, and a quadrupole mass spectrometer.

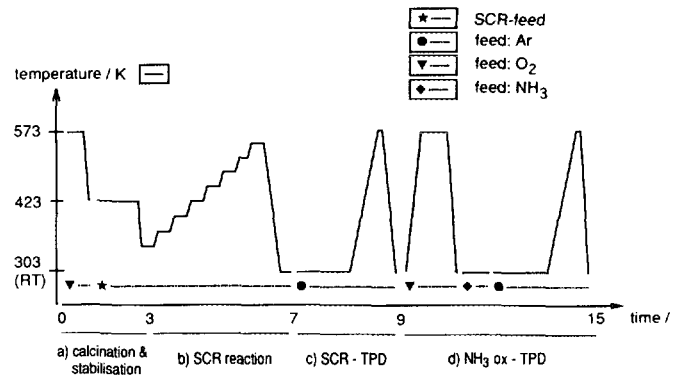

FIG. 2. Schematic presentation of experimental procedure. Changes of temperature and composition of gas flow as a function of time are illustrated. The symbols designate the different gas flows passing through the sample, as identified in the inset (cf. text, experimental section).

sample was calibrated by locating a second thermocouple directly in the sample powder during measurement. On the basis of this calibration experiment the actual temperature of the sample could be estimated.

The concentration of the desorbing gas was monitored with the mass spectrometer. The temperature of the recipient was kept at 363 K. The following gas mixtures (Carbagas) were used directly as calibration gas and for the mixing of the reactant feed gas: 3600 ppm NH_3 in Ar, 3590 ppm NO in Ar, 7.2% O_2 in Ar, 1980 ppm N_2O in Ar, and 3300 ppm N_2 in Ar.

Argon (99.999%) was dried over hydrosorb and oxysorb (Griesheimer). The gas flow was kept constant at 50 ml (STP) min^{-1}. SCR feed gas (900 ppm NH_3, 900 ppm NO, 1.8% O_2, balance Ar) was mixed by flow controllers (Brooks).

For kinetic measurements the DRIFT cell was substituted by a heatable U-tube reactor with an i.d. of 3.6 mm, as described in a previous report (23). The measurements were carried out using the 120–300-μm sieve fraction of the mechanically agglomerated aerogel materials and adjusting the sample mass in such a way that a gas hourly space velocity (GHSV) of 24,000 h^{-1} was established.

The experimental procedure is shown schematically in Fig. 2. During the entire procedure the composition of the gas mixture passing the sample was monitored by mass spectroscopy. Before changing the gas mixture, the new feed gas composition was checked by mass spectroscopy without passing it over the sample. For recording the background spectra, the sample was calcined for 1 h at 573 K in 7.2% oxygen, and then cooled to 423 K (Fig. 2, step a). At this temperature 200 scans were detected by FTIR against a KBr reference at a spectral resolution of 8 cm^{-1}. At the same temperature, the gas flow was switched to the SCR feed gas mixture. After steady-state behaviour had been attained, the sample was cooled to 373 K.

After this procedure, the temperature was raised stepwise (50 K) in the following manner (Fig. 2, step b). First the temperature was rapidly increased by 50 K, using a ramp rate of 7 K min^{-1}. Thereafter, the temperature was held constant for 30 min. After steady state had been attained, the conversion was determined and 200 FTIR spectra were accumulated at a resolution of 8 cm^{-1}. The cycle was repeated until a final temperature of 573 K was reached.

Subsequently, for the *SCR–TPD* experiments (Fig. 2, step c) the gas feed was switched to argon. In order to remove the physisorbed species, Ar was passed over the catalyst for 2 h at room temperature. In the following TPD experiment, the temperature was increased from 298 to 573 K at a rate of 7 K min^{-1}. Fifty scans were accumulated over a temperature interval of 25 K in order to obtain an adequate signal-to-noise ratio. As the desorption is a dynamic process, the obtained spectrum represents an average over the temperature interval of 25 K. In the following these spectra are labelled with the initial interval temperature.

For the *NH_3 ox–TPD* experiments (Fig. 2, step d), the catalysts were pretreated again for 1 h at 573 K under an atmosphere containing 7.2% oxygen. After this oxidation, the samples were exposed to 3600 ppm NH_3 in Ar (50 ml (STP) min^{-1}) for 30 min. The physisorbed ammonia was removed by flushing with pure argon for 120 min. Otherwise the same procedure was applied as for the SCR–TPD.

Transient measurements were carried out under reaction conditions at 473 K. FTIR spectra (100 scans, 4 cm^{-1}) were recorded during successive intervals of 7.5 min. During the whole experiment the product gas was monitored by mass spectrometry.

All FTIR spectra are ratioed with respect to the background spectrum of the unloaded catalyst, to isolate the spectra of the adsorbed species. From the ratioed spectrum R/R_0, the Kubelka–Munk function $f(R/R_0)$ was calculated.

RESULTS

Structural and Catalytic Properties of the Aerogel Catalysts

The crystalline fraction of all aerogel powders was made up of anatase crystallites with mean sizes of 7.3–7.5 nm. They all showed a type-IV isotherm with a type-H1 hysteresis according to IUPAC classification. After calcination in air at 573 K the following BET surface areas (m^2 g^{-1}) were measured: titania, 182; 5 wt% vanadia–titania, 194; 10 wt% vanadia–titania, 183; 20 wt% vanadia–titania, 192. Note that especially the surface areas of the binary oxides are considerably higher than those generally observed with conventionally prepared mixed oxides of these constituents (24). Moreover, they all show pronounced meso- to macroporosity and only a little microporosity. The specific nitrogen pore volumes range from 0.71 to 1.0 cm^3 g^{-1} and the specific micropore surface areas estimated from the corresponding *t*-plot analysis amount to 10–13 m^2 g^{-1}. Otherwise, the mechanical agglomeration of these aerogel powders for the kinetic studies did not cause significant changes in their textural characteristics.

Kinetic measurements carried out under the standard conditions given in the experimental section showed that the activity of the vanadia–titania aerogels increased with higher vanadia content. This is reflected by the temperatures necessary to reach 50% NO conversion (T_{50}), which were 545 K for 5 wt% vanadia–titania, 470 K for 10 wt% vanadia–titania, and 440 K for 20 wt% vanadia–titania. Pure titania did not show significant NO conversion activity in this temperature range. A detailed consideration of kinetic measurements will be reported elsewhere (22).

Titania Aerogel—NH_3 Desorption after Oxidative Pretreatment (Fig. 2, Step d)

Subsequent to NH_3 adsorption on a titania aerogel, preoxidised as described in the experimental section (Fig. 2, step d), IR spectra were recorded during the temperature-programmed desorption of ammonia. Seven major bands in the range between 1300 and 4000 cm^{-1} are discernible in the top spectrum of Fig. 3 recorded at 298 K. We recall that the Kubelka–Munk function $f(R/R_0)$ was calculated with respect to the background spectrum (R_0) of the unloaded catalyst surface. Positive bands are therefore due to the chemisorption of ammonia, whereas the negative signals indicate a consumption of surface hydroxyl groups. Bands at 3400 and 3350 cm^{-1} are assigned to the asymmetric and symmetric stretching modes of chemisorbed ammonia, respectively (15). The intense signal at 3260 cm^{-1} and the band at 3155 cm^{-1} are due to a Fermi interaction between these stretching modes and the overtone of the asymmetric NH_3 deformational vibration (12). Further characteristic bands at lower frequencies are the asymmetric deformational vibration of Lewis-bound ammonia at 1600 cm^{-1} and the ν_2(E) band of Brønsted-bound ammonia at 1670 cm^{-1} (9, 14). A peak at 1480 cm^{-1} has been assigned to the NH_2 scissoring mode (25, 26).

Species desorbing during the described experiment, as monitored by the respective mass spectrometric signals, are shown in the right panel of Fig. 3. Ammonia exhibits a maximum desorption rate at 370 K, with a gradual tailing towards higher temperatures. A slight desorption of water is observed with increasing temperature; no other desorbing species are detected.

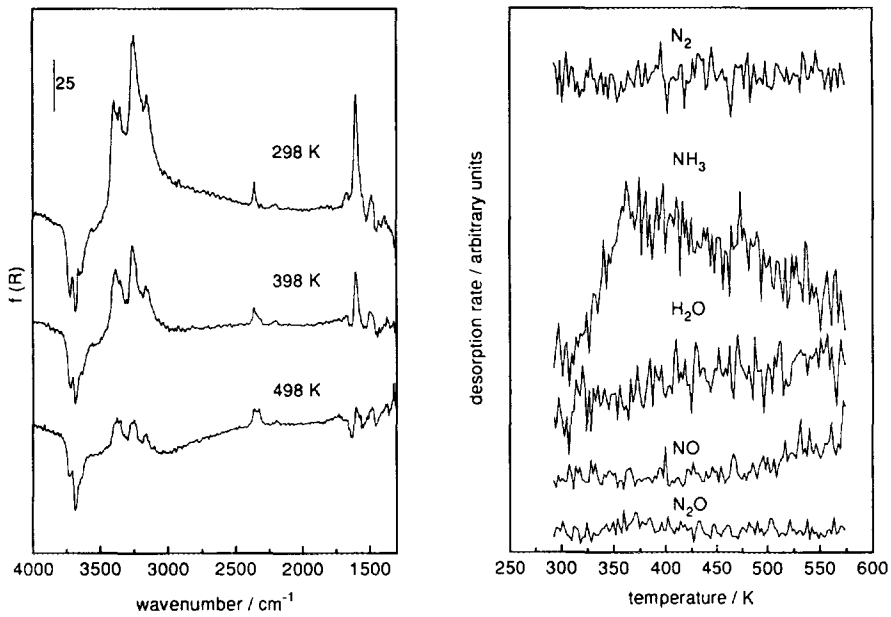

FIG. 3. Ammonia desorption from titania aerogel after preoxidation and ammonia exposure (*NH_3 ox–TPD;* Fig. 2, step d). Left panel: DRIFT spectra at different temperatures; right panel: TPD monitored by mass spectrometry.

Titania Aerogel–TPD after SCR Pretreatment (Fig. 2, Step c)

When a titania sample loaded with SCR feed gas is heated in argon, the changes in the surface FTIR spectra shown in Fig. 4 are observed. Peaks at 3400, 3350, 3260, and 3155 cm^{-1} are assigned as in Fig. 3. A broad band extending from 2600 to 3200 cm^{-1} is due to Brønsted-bound ammonia (14). In the spectral region below 2000 cm^{-1}, peaks at 1660 and 1440 cm^{-1} are assigned to ν_2(E) and ν_4(F) deformational motions of NH_3 bound to Brønsted sites. The band at 1606 cm^{-1} observed in the 298 K spectrum represents a superposition of the deformation vibration of Lewis-bound ammonia at 1600 cm^{-1}

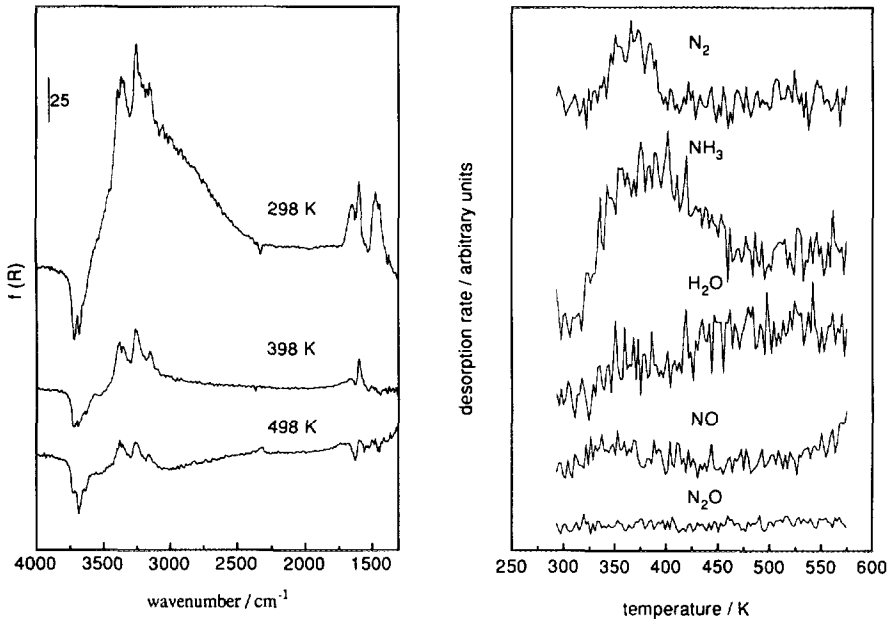

FIG. 4. Ammonia desorption from pure titania aerogel after exposure to SCR conditions (*SCR–TPD;* Fig. 2, step c). Left panel: DRIFT spectra at different temperatures; right panel: TPD monitored by mass spectrometry.

and a band at 1610 cm^{-1} assigned to chemisorbed nitrate ions (9, 11, 14). The weak peak at 1480 cm^{-1} is assigned to an NH_2 scissoring mode, as in Fig. 3. With increasing temperature, all peaks, particularly those of adsorbed ammonia, are decreasing in intensity.

The corresponding mass spectrum in the right panel of Fig. 4 shows nitrogen desorption, with a maximum at 360 K, whereas a slight decreasing water desorption, starts at 340 K. Ammonia desorption starts at about 320 K, reaches a maximum around 380 K, and then decreases gradually up to 573 K.

Vanadia–Titania Aerogels—NH_3 Desorption after Oxidative Pretreatment (Fig. 2, Step d)

The DRIFT spectrum recorded on the 20 wt% vanadia–titania aerogel at 298 K (Fig. 5) exhibits a dominant peak at 1435 cm^{-1} assigned, as above, to the ν_4(F) bending mode of Brønsted-bound ammonium (9, 11, 14); the corresponding ν_2(E) vibration is seen as a shoulder at 1660 cm^{-1}. The strong signal at 1602 cm^{-1} is due to Lewis-bound ammonia (14). In the spectrum recorded at 398 K, all peaks including the one at 1600 cm^{-1} appear with decreased intensity. Only weak signals at 1600 and 1435 cm^{-1} remain observable at the highest temperature of 498 K; signals due to Lewis-bound and Brønsted-bound ammonia are also detected in the 2500–3500 cm^{-1} region.

The corresponding mass spectrum, in the right panel of Fig. 5, shows the expected ammonia desorption, with a maximum rate at about 380 K. Above 430 K, a small amount of nitrogen desorption is observed; water is released with increasing rate over the entire temperature range studied. No desorption of NO or N_2O is detected within experimental error.

Vanadia–Titania Aerogels—TPD after SCR Pretreatment (Fig. 2, Step c)

The DRIFT spectra recorded during *SCR–TPD* (Fig. 6) are similar to those observed during the TPD of ammonia (Fig. 5). At 298 K, the intensity of the 1435 cm^{-1} band is even larger than the corresponding signal in Fig. 5. In the mass spectrum (right panel in Fig. 6), the most prominent difference with respect to *NH_3–TPD* is a pronounced maximum of water desorption observed at 370 K, which is followed by a continuous rise between 450 and 573 K.

Influence of the Vanadia Content

Changes in the adsorbate concentrations due to the presence of vanadia are seen clearly in Fig. 7: the spectra recorded during *SCR–TPD* at a temperature of 398 K are compared for three catalysts containing 5, 10, and 20 wt% of vanadia, respectively. The fraction of Brønsted-bound ammonia, as judged from the signal intensities at 1435 and 1660 cm^{-1}, increases significantly with higher vanadia content. Furthermore, in the spectrum of the 20 wt% vanadia–titania catalyst, a new peak at 1750 cm^{-1} is detected. Kugler *et al.* (27) have assigned this frequency to the asymmetric stretching mode of an NO dimer, i.e., O=N–N=O.

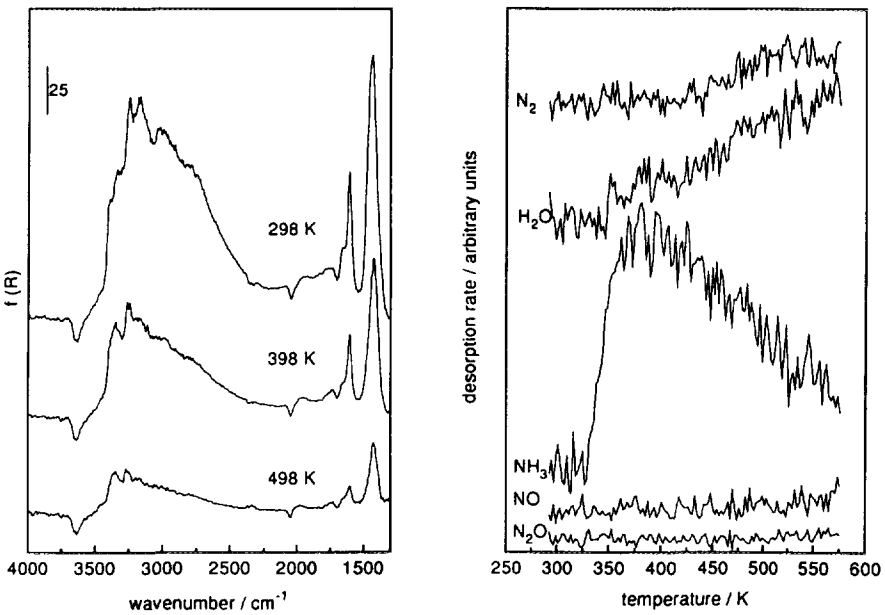

FIG. 5. Ammonia desorption from 20 wt% vanadia–titania aerogel after oxidative pretreatment (*NH_3 ox–TPD;* Fig. 2, step d). Left panel: DRIFT spectra at different temperatures; right panel: TPD monitored by mass spectrometry.

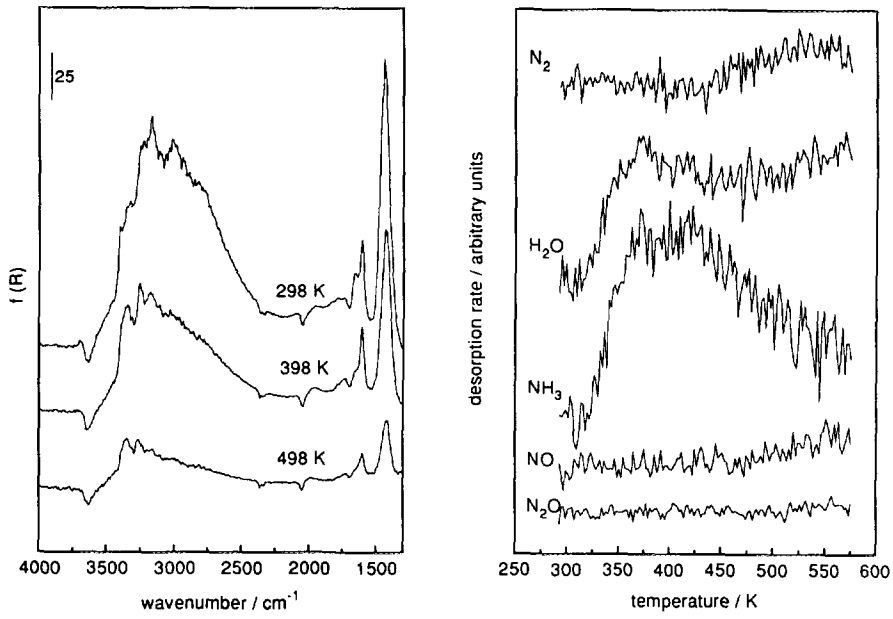

FIG. 6. Ammonia desorption from 20 wt% vanadia–titania aerogel after SCR pretreatment (*SCR–TPD;* Fig. 2, step c). Left panel: DRIFT spectra at different temperatures; right panel: TPD monitored by mass spectrometry.

Transient Experiments

In a first run, the aerogel catalyst containing 20 wt% of vanadia was initially exposed to the SCR feed gas (50 ml min^{-1}) at 473 K for 30 min. Subsequently, the ammonia concentration in the reactant flow was reduced to zero, and time-dependent changes were observed both in FTIR and in mass spectra (Fig. 8). The strong signals due to Brønsted-bound ammonia (in particular, the signal at 1435 cm^{-1}) are seen to decrease as a function of time. In contrast, the OH stretching mode at 3680 cm^{-1}, which is negative with respect to the background of the unloaded catalyst in the spectrum recorded at $t = 0$, has changed sign after 7.5 min, indicating that OH groups are restored on the surface. After 15 min, the signals due to Brønsted-bound ammonia have disappeared, whereas the deformation band of Lewis-bound NH_3 at 1602 cm^{-1} persists. Analysis of the desorbing product (right panel in Fig. 8) shows a decrease in the concentrations of N_2 and H_2O, and an increasing signal due to NO in the product gas.

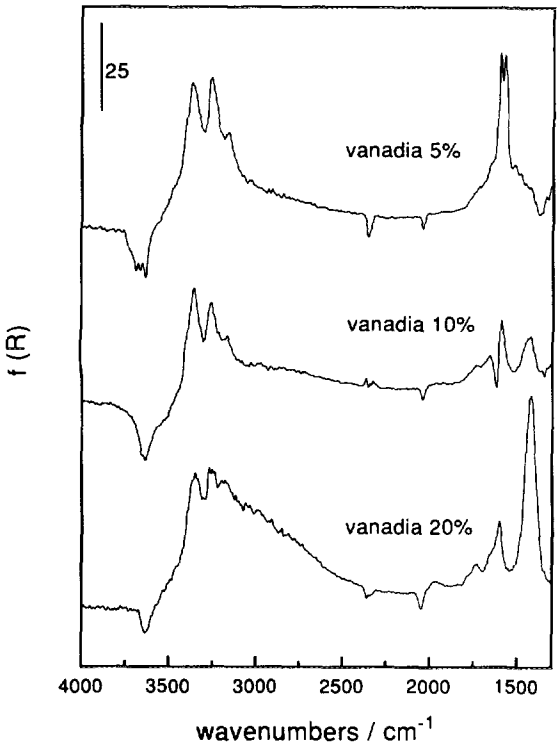

FIG. 7. Effects of vanadia content of the different vanadia–titania aerogels on *in situ* DRIFT spectra during the SCR of NO at 473 K.

In the second experiment, the catalyst was first exposed to a flow of 3600 ppm NH_3 in argon (50 ml min^{-1}) at 473 K for 30 min. Subsequently, the reactant mixture was changed to 900 ppm NO and 18,000 ppm O_2 in argon, which corresponds to the SCR feed with ammonia omitted. The DRIFT experiments (Fig. 9, left panel) show the same temporal development as described above for the catalyst that had been preconditioned under SCR reaction conditions (Fig. 8). A remarkable exception is the disappearance of the band at 1750 cm^{-1} due to the NO dimer in the absence of ammonia (Fig. 9). Product analysis (right panel) shows a sudden rise in the concentrations of N_2 and H_2O after exposing the NH_3-loaded catalyst to the mixture containing NO and O_2. After a time of 5 min, the

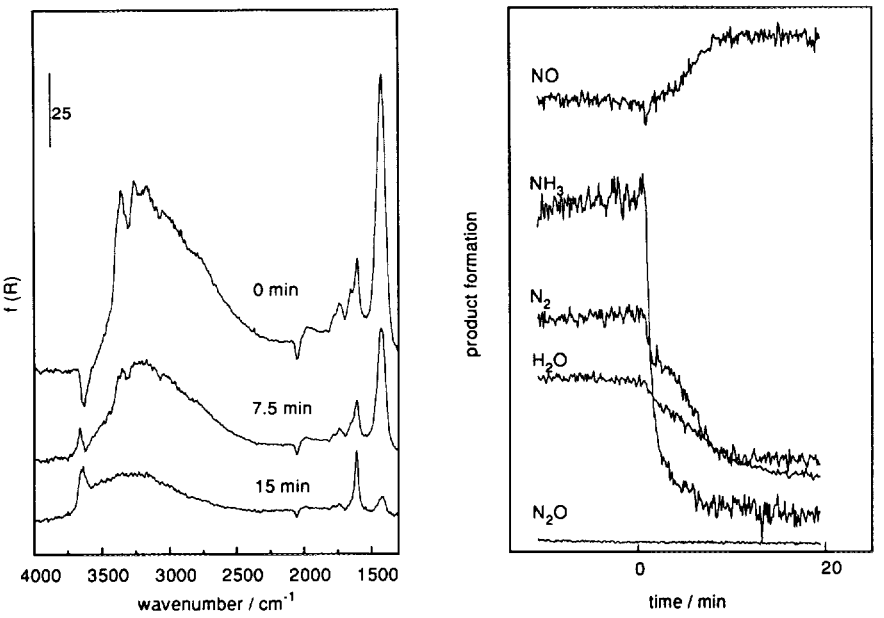

FIG. 8. Transient experiment with omission of NH_3. After steady-state conditions had been established under SCR feed at 473 K for the 20 wt% vanadia–titania aerogel, the ammonia was substituted by argon at $t = 0$. Left panel: DRIFT spectra at different times; right panel: desorbing species monitored by mass spectrometry.

signals due to these products are observed to decrease again, whereas the concentration of unconverted NO is increasing.

Finally, in the third experiment, the catalyst was first exposed to the SCR feed *at 473 K* for 30 min, subsequently, the oxygen concentration in the reaction mixture was rapidly reduced to zero. No changes in the DRIFT spectra are observed subsequent to this step (Fig. 10). In the product gas stream (right panel), the concentrations of the N_2 and H_2O products are observed to decrease, and the signal due to unreacted NO increases; substantial amounts of NH_3 start to desorb some 10 min later.

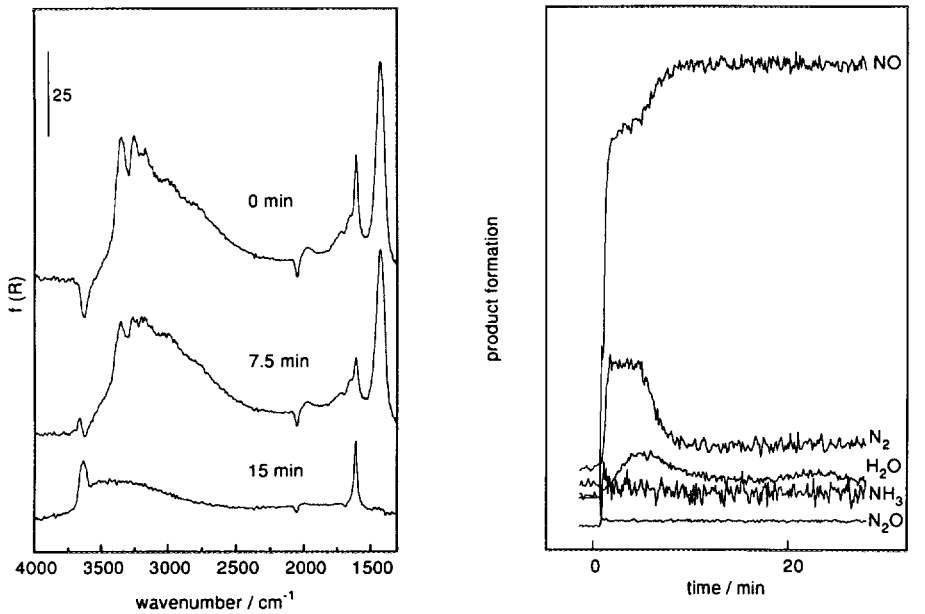

FIG. 9. Effect of activity of preadsorbed ammonia—switch from NH_3/Ar to NO/O_2/Ar feed. After the 20 wt% vanadia–titania aerogel had been loaded with ammonia at 473 K, the flow was changed to 900 ppm NO and 18,000 ppm O_2 (balance Ar) at $t = 0$. Left panel: DRIFT spectra at different times; right panel: desorbing species monitored by mass spectrometry.

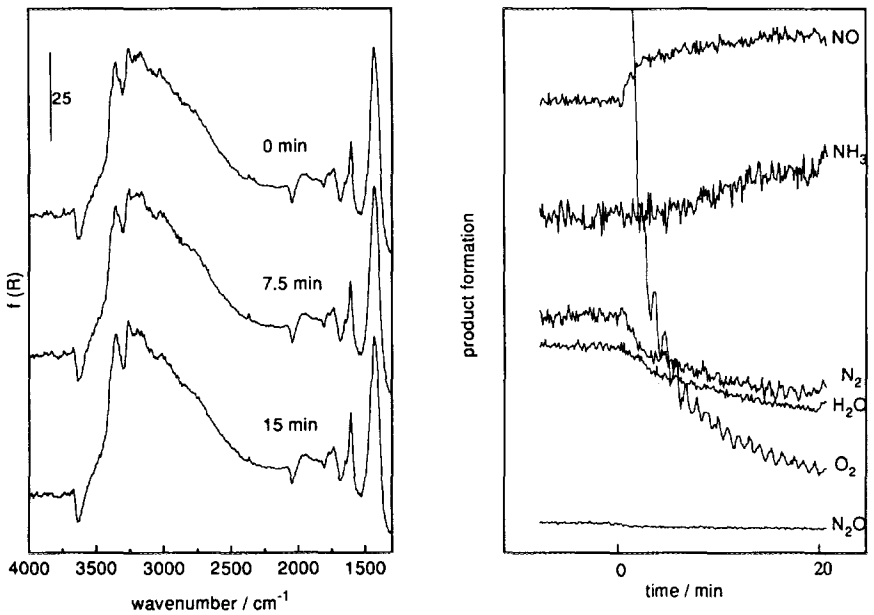

FIG. 10. Transient experiment with omission of oxygen—effect of absence of oxygen. After steady-state conditions had been established with the 20 wt% vanadia–titania aerogel under SCR feed at 473 K, the oxygen was substituted by argon at $t = 0$. Left panel: DRIFT spectra at different times; right panel: desorbing species monitored by mass spectrometry.

DISCUSSION

Adsorbed Species

On the pure titania aerogel, mainly Lewis-bound ammonia is observed subsequent to NH_3 adsorption at room temperature (Fig. 3); bands due to Brønsted-bound NH_3 are comparatively weak. In contrast, on the vanadia–titania aerogels bands due to the two types of binding are comparable in intensity.

In addition, bands due to adsorbed NO are detected on the pure titania aerogel. The corresponding signal becomes observable in our DRIFT spectra as a consequence of the high surface area, as compared to conventional catalyst supports. These results are in agreement with coadsorption experiments of Ramis *et al.* (9, 12) and Topsøe (14); binding of NO on titania surfaces has also been observed by Odriozola *et al.* (8).

TPD Experiments

On pure titania subjected to *oxidative* pretreatment, surface hydroxyl groups are only partly restored upon ammonia desorption (Fig. 3), as water would be required to replenish the OH concentration. In *SCR–TPD* (Fig. 4), desorption of both N_2 and H_2O is observed. N_2 shows a peak at 360 K and H_2O starts desorption at 340 K. From this observation we conclude that NO and NH_3, which have both been adsorbed during catalyst conditioning in SCR feed, are reacting while the catalyst temperature is being raised in a stream of argon. At 398 K, only Lewis-bound ammonia is observed to reside on the surface. According to the mass spectra (Fig. 4), the latter species desorbs between 320 K and 573 K. Taken together, these observations suggest that a reaction between Brønsted-bound ammonia and adsorbed NO is responsible for the formation of N_2 and H_2O *over pure titania.*

On the vanadia–titania aerogels (Figs. 5 and 6), the signals due to Brønsted-bound ammonia are dominant in intensity; they exhibit a modest decrease up to 398 K and a more extensive depletion at higher temperatures. According to the mass spectra, only NH_3 and H_2O are desorbing below 398 K in the TPD experiments where the loaded catalysts are heated in a stream of argon. This may be a consequence of the fact that NO adsorption is not observed on these catalysts. Incipient desorption of N_2 is detected above 450 K. At these temperatures, adsorbed NH_3 might react with surface hydroxyl groups to some extent to form N_2 and H_2O. Similar results have been reported for commercial vanadia–titania catalysts by Went and Bell (13), Topsøe (14), and Ramis *et al.* (9, 12). Thus in this respect there are no pronounced differences between the adsorption behaviour of vanadia–titania aerogels and that of catalysts where vanadia is supported on lower surface area titania materials, such as TiO_2 P25 (Degussa).

Transient Experiments

The increase in SCR activity with increasing vanadia content, as discussed above, may be directly correlated

with the changes in the DRIFT spectra observed during SCR–TPD, as shown in Fig. 7. The signal intensity of Brønsted-bound ammonia residing on the surface at 398 K increases significantly with the vanadia content.

When ammonia is omitted from the feed (Fig. 8), a slow decrease of the NO conversion is observed. The concentrations of the products, N_2 and H_2O, are decreasing over a period of $\approx$10 min, whereas the concentrations of Brønsted-bound ammonia and of the adsorbed NO dimer are decreasing as deduced from the DRIFT spectra; at the same time the regeneration of surface hydroxyl groups is observed.

In the complementary experiment where a surface is first precovered with ammonia and then exposed to an SCR feed without NH_3 (Fig. 9), a burst of N_2 and H_2O products is observed while the adsorbed ammonia is consumed. Subsequently, the product concentrations are decreasing slowly over a time of 5 min while the effluent concentration of unreacted NO is increasing, as above.

Finally, when oxygen is omitted from the SCR feed (Fig. 10), no changes in the concentrations of observed surface species are observed. However, as the proper oxidation state of the surface is not maintained under an $NO/NH_3/Ar$ feed in the absence of oxygen, the turnover decreases: An increasing amount of NO and NH_3 feed gas passes through the catalyst sample without reacting, whereas the concentrations of the N_2 and H_2O products are decreasing.

CONCLUSIONS

Both the spectra recorded during the TPD experiments and the transient experiments show that Brønsted-bound ammonia is involved in the SCR reaction, in contrast to the conclusions of Ramis *et al.* (9). Products are not formed when a catalyst loaded under SCR feed is subsequently heated in pure argon; this implies that NO is not held in significant concentrations on the surface of vanadia–titania catalysts. In agreement with this statement, the bands of the adsorbed NO species, if observed, appear always weak.

These findings are consistent with an Eley–Rideal-type mechanism. The transient experiment in which NH_3 was omitted from the SCR feed (still containing NO) shows that the IR band due to species originating from NO adsorption decreases in parallel with that of Brønsted-bound ammonia. This result is in agreement with the suggestion of Janssen *et al.* (5) that the binding of NO to adsorbed ammonium ions is the first step of an Eley–Rideal-type mechanism. The high IR intensity of the 1660 cm^{-1} band may be taken as further support for this model. This deformational vibration $\nu_2(E)$ is not IR active (28) in the free ammonium ion, but becomes observable upon binding of the latter to solid supports. Coordination of an ammonium ion to the vanadia as proposed would distort the tetrahedral geometry, and hence tend to enhance the intensity of the 1660 cm^{-1} deformational mode. However, Odriozola *et al.* (8) report weak adsorption of NO on a reduced vanadia surface. This is very difficult to observe under reaction conditions using DRIFT.

Upon exposure of titania-supported vanadia to SCR conditions, ammonia reduces the vanadia surface partially, as was recently shown by *in situ* XPS measurements on model catalysts (29). Since NO adsorption on these reduced sites seems to be possible (8), contributions via a Langmuir–Hinshelwood mechanism cannot be ruled out on a partially reduced vanadia surface.

ACKNOWLEDGMENT

Financial support of this work by the Swiss National Science Foundation (NFP 24) is gratefully acknowledged.

REFERENCES

1. Bosch, H., and Janssen, F., *Catal. Today* **2,** 369 (1988).
2. Takagi, M., Kawai, T., Soma, M., Onishi, T., and Tamuru, T., *J. Phys. Chem.* **80,** 430 (1976).
3. Takagi, M., Kawai, T., Soma, M., Onishi, T., and K. Tamaru, *J. Catal.* **50,** 441 (1977).
4. Imomata, M., Miyamoto, A., and Murakami, Y., *J. Catal.* **62,** 140 (1980).
5. Janssen, F. J. J. G., Van den Kerkhof, F. M. G., Bosch, H., and Ross, J. R. H., *J. Phys. Chem.* **91,** 6633 (1987).
6. Chen, J. P., and Yang, R. T., *J. Catal.* **125,** 411 (1990).
7. Gasior, M., Haber, J., Machej, T., and Czeppe, T., *J. Mol. Catal.* **43,** 359 (1988).
8. Odriozola, J. A., Heinemann, H., Somorjai, G. A., De la Banda, J. F. G., and Pereira, P., *J. Catal.* **119,** 71 (1989).
9. Ramis, G., Busca, G., Bregani, F., and Forzatti, P., *Appl. Catal.* **64,** 259 (1990).
10. Morishige, K., Kittaka, S., Katsuragi, S., and Mirimoto, T., *J. Chem. Soc., Faraday Trans. 1* **78,** 2947 (1982).
11. Busca, G., *Langmuir* **2,** 577 (1986).
12. Ramis, G., Busca, G., Lorenzelli, V., Forzatti, P., *Appl. Catal.* **64,** 243 (1990).
13. Went, G. T., and Bell, A. T., *Catal. Lett.* **11,** 111 (1991).
14. Topsøe, N.-Y., *J. Catal.* **128,** 499 (1991).
15. Topsøe, N.-Y., Slabiak, T., Clausen, S. B., Srnak, T. Z., and Dumesic, J. A., *J. Catal.* **134,** 742 (1992).
16. Srnak, T. Z., Dumesic, J. A., Clausen, B. S., Törnqvist, E., and Topsøe, N.-Y., *J. Catal.* **135,** 246 (1992).
17. Went, G. T., Leu, L.-J., Rosin, R. R., and Bell, A. T., *J. Catal.* **134,** 492 (1992).
18. Nickl, J., Dutoit, D., Baiker, A., Scharf, U., and Wokaun, A., *Ber. Bunsenges. Phys. Chem.* **97,** 217 (1993).
19. Dines, T. J., Rochester, C. H., and Ward, A. M., *J. Chem. Soc., Faraday Trans.* **87,** 1473 (1991).
20. Dines, T. J., Rochester, C. H., and Ward, A. M., *J. Chem. Soc., Faraday Trans.* **87,** 1611 (1991).
21. Schneider, M., and Baiker, A., *J. Mater. Chem.* **2,** 587 (1992).
22. Schneider, M., Maciejewski, M., Tschudin, S., Wokaun, A., and Baiker, A., submitted for publication.

23. Curry-Hyde, E., and Baiker, A., *Ind. Eng. Chem. Res.* **29,** 1985 (1990).
24. Handy, B. E., Maciejewski, M., and Baiker, A., *J. Catal.* **134,** 75 (1992).
25. Miyata, H., Mukai, T., Ono, T., and Kubokawa, Y., *J. Chem. Soc., Faraday Trans. I* **84,** 4137 (1988).
26. Knözinger, H., *Adv. Catal.* **25,** 184 (1976).
27. Kugler, E. L., Kadet, A. B., and Gryder, J. W., *J. Catal.* **41,** 72 (1976).
28. Davydov, A. A., "Infrared Spectroscopy of Adsorbed Species on the Surface of Transition Metal Oxides." Wiley, Chichester, 1984.
29. Schild, Ch., Nickl, J., Baiker, A., Hund, M., and Wokaun, A., *Catal. Lett.*, in press.